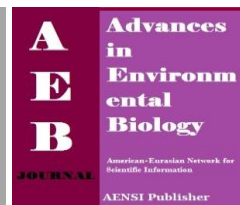




AENSI Journals

Advances in Environmental Biology

ISSN-1995-0756 EISSN-1998-1066

Journal home page: <http://www.aensiweb.com/aeb.html>

Characterizations of Thermoplastic Starch and Starch Reinforced Montmorillonite Clay Nanocomposite

¹A.R.N. Humairah, ¹A.Zuraida, ²S. Norshahida, ¹Z.S. Naqiah

¹Department of Manufacturing & Materials Engineering, Kulliyah of Engineering, International Islamic University Malaysia, Jalan Gombak, 53100, Kuala Lumpur, Malaysia

²Cluster for Polymer Composite, School of Materials and Mineral Resources Engineering, University Science Malaysia, Engineering Campus, 14300, NibongTebal, Penang, Malaysia

ARTICLE INFO

Article history:

Received 14 Feb 2014

Received in revised form 24

February 2014

Accepted 29 March 2014

Available online 14 April 2014

Key words:

Sago Starch, Montmorillonite, Extrusion, Compression Moulding, Intercalation

ABSTRACT

This paper reported the characterizations of thermoplastic starch (TPS) and starch/nanoclay composite prepared from sago (*Metroxylonrottb.*) and Montmorillonite (MMT) nanoclay. Preparation of nanocomposite using inorganic filler such as MMT is among the means to enhance some properties of starch biopolymer. The thermoplastic starch-Montmorillonite (TPS-MMT) nanocomposite was produced by plasticizing with glycerol through melt blending before being compression moulded. The investigated TPS and nanocomposite were prepared at starch/glycerol weight fraction of 70:30 with 3, 6, and 12 wt % of MMT content. The degree of crystallinity of the TPS-MMT was analyzed by X-ray Diffraction (XRD) which showed that TPS crystalline structure was affected by MMT integration while both XRD and Fourier Transform Infrared Spectroscopy (FTIR) suggested the occurrence of matrix-reinforcement intercalation. Scanning Electron Microscope (SEM) presented micrographs of continuous phase and good adhesion of TPS-MMT nanocomposite at lower clay concentration.

© 2014 AENSI Publisher All rights reserved.

To Cite This Article: A.R.N. Humairah, A. Zuraida, S. Norshahida, Z.S. Naqiah., Characterizations of Thermoplastic Starch and Starch Reinforced Montmorillonite Clay Nanocomposite. *Adv. Environ. Biol.*, 8(3), 792-796, 2014

INTRODUCTION

Plants are potential sources for replacing synthetic polymers into biopolymers due to the fact that they are renewable, ease of availability, inexpensive, edible, biocompatible, and biodegradable. Among natural polymers, starch is a promising raw material that can be converted into biodegradable thermoplastic or bioplastic under thermomechanical conditions with the presence of a plasticizer [1,2]. Research on thermoplastic from various starches has been extensively studied such as potato, corn, wheat and cassava starch [3]. Another starch alternative is sago starch, produced from the trunk of sago palms that are widely available in South East Asia. Sago palm (*Metroxylonsagu*) is among the oldest tropical plants utilized by man for its stem starch [4]. In Malaysia, sago palm is categorized under one of the potential less utilized food palms including maize and sugar palm tree. Moreover, major sago palm population in Malaysia is situated in Sarawak where the total area of growth of sago palm by 2009 was recorded to be 58 898 hectares and the export of sago products by Sarawak in 2009 was 43,102 tonne [5]. The polysaccharide chains within the starch which primarily consist of amylose and amylopectin, a linear and branched chain of glucose molecules, respectively, facilitate the formation of sago starch into TPS. The phenomenon occurred through the disruption and gelatinization of the starch polymer chains at a specific critical temperature [6].

Starch-based polymer, however, exhibits low mechanical properties, high T_g and water absorption, poor moisture barrier as well as sensitive to humidity, temperature and pH changes [7-9]. As a result, modification of TPS is required to overcome these restrictions. Recent researches have been paid attention towards nanoclay in the nanocomposite field because of their small particle size, large surface area, high aspect ratio and intercalation ability [9-12].

The produced nanocomposite with only slight addition of nanoclay (1-10%) provide satisfactory improvement in mechanical, thermal, electrical, fire retardant and barrier properties [11,13,14], which is influenced by the clay unique silicate multilayers. The optimum performance of polymer reinforced clay composite, however, is attained when the clay is uniformly dispersed in the polymer matrix.

Corresponding Author: A. Zuraida, Department of Manufacturing & Materials Engineering, Kulliyah of Engineering, International Islamic University Malaysia, Jalan Gombak, 53100, Kuala Lumpur, Malaysia
E-mail: zuraidaa@iium.edu.my

Nanoclay such as MMT can be a reinforcing phase with TPS since MMT is a layered aluminium silicate with sodium cations and allows intercalation of starch amylose and hydrophilic plasticizer within its gallery spacing [15,16]. Thus, MMT is able to provide good polarity matching with polysaccharides such as starch to form nanocomposite. In addition, MMT is one of the most commonly used layered silicates due to its environmentally friendly characteristic, readily obtainable in great quantity at relatively low cost [17].

The present work sets out the characterizations of TPS from sago starch plasticized with glycerol as well as plasticized starch reinforced MMT nanocomposite through x-ray diffraction, fourier infrared analysis and surface morphology. Furthermore, the ability of sago starch matrix to intercalate within the MMT gallery spacing is investigated.

MATERIALS AND METHODS

Materials:

Commercially available sago starch powder was purchased from Hup Seng Heng Sdn Bhd, Malaysia, with sieving size passing through 50 μm . Glycerol (99.5% purity) was used as a non-volatile plasticizer and supplied by Merck, Germany. The unmodified montmorillonite (MMT) nanoclay was also supplied from Merck and used as received.

Preparation of TPS and nanocomposite:

The TPS formulation was maintained at weight ratio of starch to glycerol of 70:30. The mixture was mechanically stirred and further processed in a twin screw extruder (Thermo HAAKER rheomix 600) at 130 $^{\circ}\text{C}$, 100 rpm. Then, the extrudate was granulated before being compression moulded (Technopress 40 HCB) at preheating temperature of 150 $^{\circ}\text{C}$ for 6 min and compression at 150 $^{\circ}\text{C}$ for 3 min. The compression moulded sheet, with dimensions of 150 x 150 x 2 mm was cold pressed for 2 min. For nanocomposite fabrication, MMT clay (3, 6 and 12 wt % based on weight of plasticized starch) was dispersed overnight in 10 ml of distilled water producing a gel that was added to the glycerol-plasticized starch mixture before extrusion. All of the compression moulded samples were then stored in sealed polyethylene bag under room temperature for a week prior to testing.

X-ray diffraction (XRD):

XRD (Shimadzu Diffractometer, XRD 6000) was conducted using $\text{CuK}\alpha$ radiation at 30 mA and 40 kV. The scans were performed at a scattering angle (2θ) range from 10 $^{\circ}$ to 40 $^{\circ}$ with step size of 0.02 $^{\circ}$ and at a rate of 2 $^{\circ}\text{C}/\text{min}$.

Fourier transform infrared (FTIR):

Perkin-Elmer Spectrum 200 spectrometer was used with the mode of 20 scans and 8 cm^{-1} resolution for the FTIR analysis. All spectra were scanned within the range 4000-380 cm^{-1} .

Scanning electron microscopy (SEM):

SEM (Model Quanta 200 MK2) examined the surface morphology of the nanocomposite at 17 kV and 50/60 Hz. Surface of the samples was sputter-coated with gold-palladium prior to SEM observation.

RESULTS AND DISCUSSION

X-ray diffraction:

The XRD patterns of the pressed specimens and as-received MMT are presented in Figure 1. The crystallinity and existence of intercalation or exfoliation of MMT can be investigated and hypothesized via XRD. Based on the MMT curve, a sharp peak at 6.125 $^{\circ}$ of 2θ is corresponded to the 001 lattice spacing of highly coherence MMT silicate layer [11,18]. In comparison, TPS sample without clay incorporation shows a featureless peak in the range of 1-10 $^{\circ}$ while the 001 peak of MMT is displaced to 5 $^{\circ}$ of 2θ in the TPS reinforced clay composite. The shifting is caused by glycerol intercalation between the MMT layers, as suggested by reports elsewhere [9,12,18]. During the intercalation stage, the polymer molecules entered the clay gallery spacing and would cause a shift of the diffraction peak to a lower angle [19]. This phenomenon occurred during the component blending in the extrusion process. Such incidence occurred due to the hydrophilic nature of starch and glycerol which can facilitate the penetration of polymer within the hydrophilic MMT gallery spacing [15]. In addition, the XRD patterns display broad humps for TPS and TPS-MMT at $2\theta = 20^{\circ}$ with some low intensity diffractions. The ill-defined diffraction peaks are observed in both TPS and TPS-MMT samples, indicating a low percentage of degree of crystallinity. The incorporation of MMT, however, has an effect on the crystalline structure of TPS, making the crystallization diffraction peaks of TPS-MMT are higher than TPS.

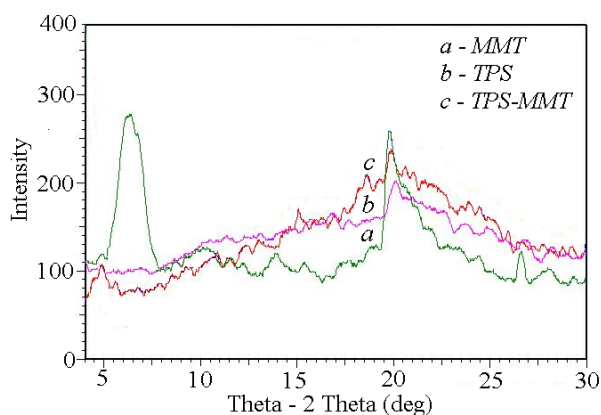


Fig. 1: XRD diffractograms of MMT, TPS and TPS-MMT nanocomposite

Fourier transform infrared (FTIR):

The FT-IR spectra of the compression moulded samples are shown in Figure 2a and 2b. Typical absorption range for O-H stretching vibration is $3700\text{--}3500\text{ cm}^{-1}$, however based on Figure 2a there is a shifting of O-H stretching peak to lower wavelength for TPS and TPS-MMT. The low absorption bands for O-H stretching vibration might be due to the intermolecular hydrogen bonds in the glycosidic ring weaken the O-H bond and lowering the band absorption region to 3200 cm^{-1} [20]. For TPS, the stretching and bending vibration of the hydrogen bonding –OH groups of starch occurs at 3280 cm^{-1} in Figure 2a and 1644 cm^{-1} in Figure 2b, respectively. The reduction of peak frequency from 3280 to 3272 cm^{-1} when the MMT is incorporated into TPS-MMTbicomposite showed that the nanoclay formed stronger interaction with TPS, since peak frequency reduced with stronger molecular interaction [21]. The characteristic peak occurred at about 1645 cm^{-1} for TPS-MMTin Figure 2b, is believed to be a feature of tightly bound water present in the starch.

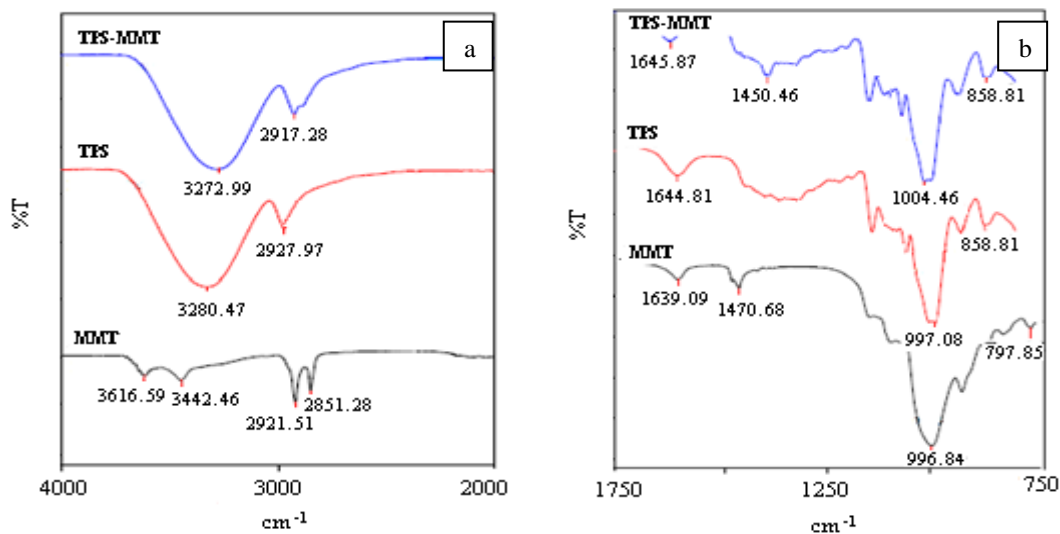


Fig. 2: FT-IR spectra of MMT, TPS and TPS-MMT at (a) higher wavenumber (cm^{-1}) and (b) lower wavenumber (cm^{-1}).

In the MMT FT-IR spectrum, the OH stretching peak, ascribed to the free hydroxyl groups, appeared at 3616 cm^{-1} and the OH stretching peak, ascribed to the hydroxyl groups that participated in the formation of hydrogen bonds appeared at 3442 cm^{-1} . When comparing between MMT and TPS-MMT spectra, however, there was only one hydroxyl groups of OH stretching peak at 3272 cm^{-1} for the latter compared with the former, which shifted to lower wavenumbers. Furthermore, an appearance of a new band for TPS-MMT sample is observed next to 2917 cm^{-1} , which is attributed to CH_2 groups [22]. Presence of glycerol in the clay galleries is confirmed with the formation of band at 1450 cm^{-1} , as supported by report elsewhere [22]. Meanwhile, the peaks at 858 cm^{-1} and 1004 cm^{-1} are attributed to the C-O bond stretching in sago starch which is almost similar with the study reported by [21].

Scanning electron microscopy (SEM):

Figure 3 compares the surface morphology of unreinforced TPS sample with reinforced composite at 6 wt % MMT and 12 wt % MMT. The SEM micrograph of TPS has a smooth and homogeneous surface representing miscibility between the starch and plasticizer due to similar polarity between the two components. The TPS continuous phase is also attributed to adequate processing parameters such as shear, pressure and temperature to fully gelatinize the starch [23]. The addition of 6 wt % MMT content as in Figure 3b formed a continuous phase suggesting the clay particles were well dispersed in the polymer matrix. Unlike the smooth surface of the biocomposite at lower MMT content, the increment amount of MMT at 12 wt % (Figure 3c) produced rough surface with agglomeration of starch granules and clay platelets. The micrograph showed a weak interaction between the clay and the starch polymer matrix that may break upon loading. It can be postulated that the incorporation of low clay content into TPS is more compatible than at higher concentration.

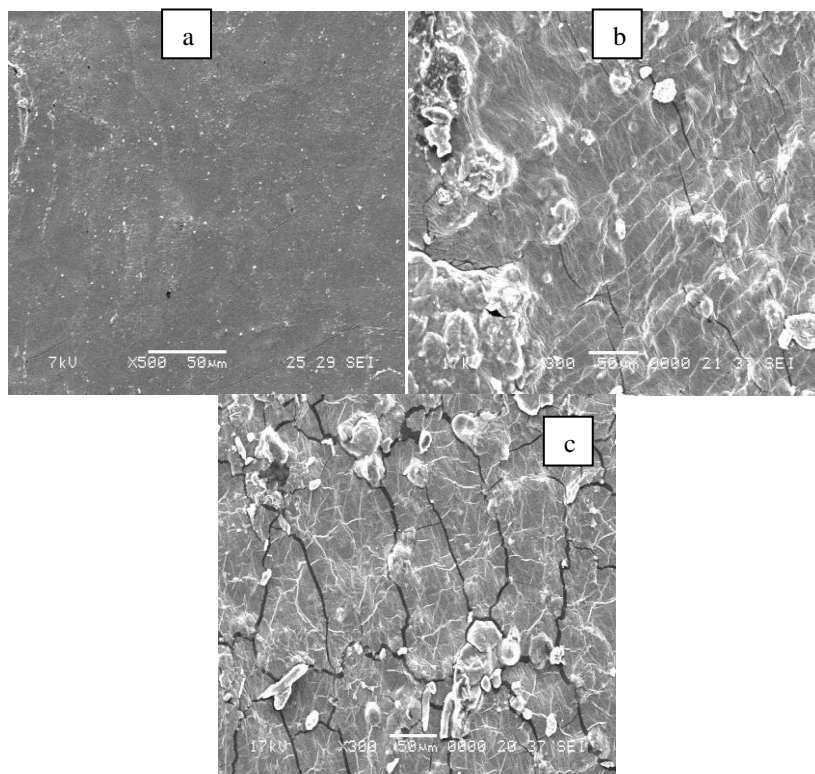


Fig. 3: SEM micrograph of a) TPS, b) TPS-6 wt % MMT and c) TPS-12 wt % MMT nanocomposite.

Conclusions:

In this research, the effect of MMT incorporation in TPS was studied and XRD patterns showed the peak of MMT was displaced to $5^{\circ}=2\theta$ from 6.125° in the TPS reinforced clay nanocomposite. The shifting was caused by glycerol intercalation between the MMT silicate layers. The FT-IR spectra suggested the occurrence of intercalation with the presence of new band at 1450 cm^{-1} . Meanwhile, the SEM micrographs revealed that lower MMT content seems to be compatible in TPS to form well-dispersed phase of nanocomposite. Thus, the findings proved the addition of MMT posed favourable interaction with TPS from sago starch plasticized glycerol.

REFERENCES

- [1] Zuraida, A., A.R.N. Humairah, A.W.N. Izwah, Z.S. Naqiah, 2012. The study of glycerol plasticized thermoplastic sago starch. *Advanced Material Research*, 576: 289-292.
- [2] Curvelo, A.A.S., A.J.F. de Carvalho and J.A.M. Agnelli, 2001. Thermoplastic starch-cellulosic fibers composite: preliminary results. *Carbohydrate Polymers*, 45: 183-188.
- [3] Prachayawarakorn, J., P. Sangnitdej, P. Boonpasith, 2010. Properties of thermoplastic rice starch composite in forced by cotton fiber or low-density polyethylene. *Carbohydrate Polymer*, 81(2): 425-433.
- [4] Lang, A.T.P., 2004. *Physico-chemical properties of starch in sago palm (metroxylonsagu) at different growth stages*, Master's thesis, Universiti Sains Malaysia.

- [5] Sarawak Agriculture Statistics, 2000-2009, 2011. Department of Agriculture Sarawak. Retrieved from <http://www.doa.sarawak.gov.my/modules/web/page.php?id=102> (8/12/11).
- [6] Omar, N., A.R.N. Humairah, M. Akmal, Z. Ahmad, 2011. Sago, its properties and applications: A review. In Ahmad, Z. (Ed.). *Sago (MetroxylonRottb.) and Its Applications*. Kuala Lumpur: IIUM Press, 8.
- [7] Azeredo, H.M.C. de., 2009. Nanocomposite for food packaging applications. *Food Research Int.*, 42: 1240-1253.
- [8] Chung, Y.L., S. Ansari, L. Estevez, S. Hayrapetyan, E.P. Giannelis, M.H. Lai, 2010. Preparation and properties of biodegradable starch-clay nanocomposite. *Carbohydrate Polymer*, 79: 391-396.
- [9] Liu, H., D. Chaudhary, S. Yusa, M.O. Tade, 2011. Glycerol/starch/Na⁺-montmorillonitenanocomposite: XRD, FTIR, DSC and HNMR study. *Carbohydrate Polymer*, 83: 1591-1597.
- [10] Alexandre, M., P. Dubios, 2000. Polymer-layered silicate nanocomposite: Preparation, properties and uses of a new class of materials. *Materials Science and Engineering R-Reports*, 28: 1-63.
- [11] Kampeerappun, P., D. Aht-ong, D. Pentrakoon, K. Srikulkit, 2007. Preparation of cassava starch/montmorillonite composite film. *Carbohydrate Polymer*, 67: 155-163.
- [12] Magalhaes, N.F., C.T. Andrade, 2009. Thermoplastic corn starch/clay hybrids: Effect of clay type and content on physical properties. *Carbohydrate Polymer*, 7: 712-718.
- [13] Avella, M., J.J. De Vlieger, M.E. Errico, S. Fischer, P. Vacca, M.G. Volpe, 2005. Biodegradable starch/clay nanocomposite films for food packaging applications. *Food Chemistry*, 93: 467-474.
- [14] Xiong, H.G., S.W. Tang, H.L. Tang, P. Zou, 2008. The structure and properties of a starch-based biodegradable film. *Carbohydrate Polymer*, 71(2): 263-268.
- [15] Chiou, B.S., D. Wood, E. Yee, S.H. Imam, G.M. Glenn, W.J. Orts, 2007. Extruded starch-nanoclaynanocomposite: Effect of glycerol and nanoclay concentration, *Polymer Engineering and Science*, 47(11): 1898-1904.
- [16] Muller, C.M.O., J.B. Laurindo, F. Yamashita, 2011. Effect of nanoclay incorporation method on mechanical and water vapour barrier properties of starch-based films. *Industrial Crop Products*, 33: 605-610.
- [17] Cyras, V.P., L.B. Manfredi, M.T. Ton-That, A. Vazquez, 2008. Physical and mechanical properties of thermoplastic starch/montmorillonitenanocomposite films. *Carbohydrate Polymers*, 73: 55-63.
- [18] Chen, B., J.R.G. Evans, 2005. Thermoplastic starch-clay nanocomposite and their characteristics. *Carbohydrate Polymer*, 61: 455-463.
- [19] Gao, W., H. Dong, H. Hou, H. Zhang, 2011. Effects of clays with various hydrophilicities on properties of starch-clay nanocomposite by film blowing. *Carbohydrate Polymer*, doi:10.1016/j.carbpol.2011.12.011.
- [20] Yaacob, B., M.C.I. Amin, K. Hashim, K. Abu Bakar, 2011. Optimization of reaction conditions for carboxymethylated sago starch, *Iranian Polymer Journal*, 20(3): 195-234.
- [21] Huang, M.F., J.G. Yu, X.F. Ma, 2004. Studies on the properties of montmorillonite- reinforced thermoplastic starch composite. *Polymer*, 45: 7017-7023.
- [22] Wilhelm, H.M., M.R. Sierakowski, G.P. Souza, F. Wypych, 2003. Starch films reinforcedwith mineral clay. *CarbohydratePolymer*, 52: 101-110.
- [23] Ma, X.F., J.G. Yu, J.J. Wan, 2006. Urea and ethanolamine as a mixed plasticizer for thermoplastic starch. *Carbohydrate Polymer*, 64: 267-273.